frontiers in Materials

REVIEW
published: 28 October 2020
doi: 10.3389/fmats.2020.586496

Optical Fiber Integrated Functional Micro-/Nanostructure Induced by Two-Photon Polymerization

Cong Xiong[1,2], Changrui Liao[1,2], Zhengyong Li[1,2], Kaiming Yang[1,2], Meng Zhu[1,2], Yuanyuan Zhao[1,2] and Yiping Wang[1,2]*

[1]Guangdong and Hong Kong Joint Research Centre for Optical Fiber Sensors, Shenzhen University, Shenzhen, China, [2]Key Laboratory of Optoelectronic Devices and Systems of Ministry of Education and Guangdong Province, College of Physics and Optoelectronic Engineering, Shenzhen University, Shenzhen, China

Owing to the limitation of optical fiber materials and conventional fabrication methods, the development of optical fiber devices has encountered a bottleneck. Recently, two-photon polymerization technology is attracting increasing research interest due to its superiorities of high precision, flexibility and diversity of polymer materials. The optical fiber integrated micro-/nanostructures induced by two-photon polymerization have become a research hotspot due to the great application expansion of optical fiber device. In this paper, we review the research progress in the field of optical fiber integrated micro-/nanostructures induced by two-photon polymerization in the last 10 years, which are classified by micro-optics, optical waveguide device and optical micro-cavity. Furthermore, we briefly discussed the future prospects of this exciting research field.

Keywords: optical fiber, two-photon polymerization, micro-/nanostructure, micro-optics, optical waveguide device, optical micro-cavity

OPEN ACCESS

Edited by:
Duk-Yong Choi, Australian National University, Australia

Reviewed by:
Walter Caseri, ETH Zürich, Switzerland
M. E. Ali Mohsin, University of Technology Malaysia, Malaysia

****Correspondence:***
Changrui Liao
cliao@szu.edu.cn

Specialty section:
This article was submitted to Polymeric and Composite Materials, a section of the journal Frontiers in Materials

Received: *28 July 2020*
Accepted: *05 October 2020*
Published: *28 October 2020*

Citation:
Xiong C, Liao C, Li Z, Yang K, Zhu M, Zhao Y and Wang Y (2020) Optical Fiber Integrated Functional Micro-/Nanostructure Induced by Two-Photon Polymerization. Front. Mater. 7:586496. doi: 10.3389/fmats.2020.586496

INTRODUCTION

Since the invention of optical fiber, it has become one of the most extensive and powerful devices in the fields of sensing, power delivery and communication due to the advantages of ultra-compact size and low optical loss (Lee, 2003; Dianov, 2012; Richardson et al., 2013). For example, commercial quartz single-mode fiber (SMF), which transmits only one mode of light, is suitable for telecommunication and fabrication of various kinds of optical fiber devices due to its low attenuation, broadband width and low price. Multi-mode fiber (MMF) has been widely used in coupling, imaging, communication and other fields because of its ability to transmit multiple modes of light, larger core, and coupling more light power of light source. (Zhang et al., 2018; Zhang et al., 2019c; Han et al., 2020). With the rapid progress of optical sensing and communication technology, the demand of optical fiber devices with better performance and multi-purpose applications is increasing, which undoubtedly promotes the research and development of all kinds of special optical fibers. Typically, in order to meet the requirements of multi-channel transmission, multi-core fibers such as two-core fiber (TCF) and seven-core fiber (SCF) have been manufactured, which not only improves the efficiency of optical signal transmission, but also greatly improves the possibility of realizing various novel types of fiber micro-/nanostructure (Li et al., 2016b; Hou et al., 2018). The micro-/nanofiber fabricated by fused tapering and D-shaped fiber fabrication by side-polishing also provide the excitation conditions of strong optical fiber evanescent field for micro-/nanostructures such as surface plasma resonance (SPR) and whispering gallery mode (WGM).(Zhao et al., 2016; Li et al., 2019). However, due to the physical parameters such as the thermo-optical and thermal

expansion coefficients of optical fiber silica materials are not ideal, it is difficult to break through its performance of sensing sensitivity and minimum detection resolution. In addition, the micro-structure in optical fiber fabricated by conventional fabrication methods such as carbon dioxide laser irradiation (Wang, 2006, 2010), femtosecond laser ablation (Li et al., 2016b; Lin et al., 2018), polishing (Zhao et al., 2016) and chemical corrosion (Li et al., 2017b) not only has rough surface, but also has low robustness due to the subtractive manufacturing.

As an outstanding 3D printing technology, femtosecond laser induced two-photon polymerization (TPP) technology has been widely used in photonics (Liu et al., 2013; Tian et al., 2016; Nocentini et al., 2018; Hou et al., 2019; Jain et al., 2019), micromachines (Alsharif et al., 2018; Power et al., 2018), microfluidics (Wu et al., 2009; Tian et al., 2010; Wang et al., 2010), and biomedicine (Spagnolo et al., 2015; Hippler et al., 2019) thanks to its high fabrication accuracy and flexibility. Before the invention of TTP technology, photolithography technology has always occupied the dominant position in 3D printing technology (Johnson et al., 2003). In order to improve the fabrication accuracy, the fabrication methods have been developed from photolithography to electron-beam lithography (Prasciolu et al., 2003), interference lithography (Sanghera et al., 2010; Yang et al., 2012) and nano-imprint technology (Kostovski et al., 2011; Kanamori et al., 2013). However, during practical fabrication aforementioned technologies have encountered issues, such as the difficulty of processing arbitrary complex 3D structures at the nanoscale, complex process and high cost. Whereas, TTP technology can be used to directly carry out high precision and real 3D fabrication in the interior of polymer (Kawata et al., 2001), hybrid materials (Serbin et al., 2003) and organic modified ceramics (Ovsianikov et al., 2007) due to the nonlinear threshold effect in the interaction with materials that overcomes the limitation of classical optical diffraction limit. Therefore, TTP is an ultraprecize fabrication technology that integrates ultrafast laser technology, microscopic technology, CAD engineering graphics technology and photochemical material technology.

By combining TPP technology and the concept of "Lab on fiber", it is possible to develop novel fiber integrated micro/nano functional device. The high precision and flexible method provides a guarantee for the fabrication of micro-/nanostructures in small optical fiber end face or optical fiber interior. More importantly, the emerging polymer materials break the barrier of optical fiber intrinsic materials. In this paper, we review the research progress in the devices of optical fiber integrated micro-/nanostructures fabricated by TPP in the last ten years, including micro-optics, optical waveguide device and optical micro-cavity. In the end, the future prospects of such fiber integrated polymer devices are discussed.

MICRO-OPTICS

Direct fabrication of micro-optics on optical fiber not only realizes the system integration, but also reduces the optical signal loss in the transmission by using optical fiber as the medium of light transmission and collection. Conventionally, in order to fabricate micro-optics on the end face of fiber, different approaches such as laser micromachining (Presby et al., 1990; Wakaki et al., 1998), focused ion-beam milling (Schiappelli et al., 2004; Cabrini et al., 2006) and nano-imprint technology (Kostovski et al., 2011; Kanamori et al., 2013) have been proposed. Recently, the TPP has been applied to the fabrication of optical fiber integrated micro-optics, which has attracted increasing research interest due to its high fabrication resolution (<100 nm) and flexible design scheme. As one of the most common micro-optics, microlens can be polymerized directly on the optical fiber end face, and the applications of imaging, illumination, beam shaping and optical trapping have been realized. Simple microlenses, such as convergent lenses, axicon lenses were the first to be printed on end face of SMF by TPP (Cojoc et al., 2010; Liberale et al., 2010), as shown in **Figure 1A**. The versatility and feasibility of TPP were proved by the successful fabrication of different structures, and the optical tests demonstrated the good optical performances of the produced micro-structures. This paves the way for the fabrication of functional micro-/nanostructures based on optical fiber by using the competitive TPP technology. Then, this group also explored polymer lenses integrated on MMF, and the focusing and imaging with increased numerical aperture have been realized by printing parabolic microlens on MMF (Bianchi et al., 2013). With the increasing maturity of TPP technology, various polymer microlenses with ingenious optical design have been extensively explored to meet the needs of different applications. As shown in **Figure 1B**, a spherical lens with an azimuthal spiral phase plate on top was fabricated on the end face of optical fiber to generate orbital angular momentum (OAM) beams in free space (Weiss and Marom, 2016). Although the clear donut shape of OAM beams did not been produced due to the scattering and absorption of light at the 0-2π transition, it could be remedied in a future run by printing a larger focal length and larger aperture lens or improving the surface quality of the transition step. It is worth noting that this method enriches the techniques for generating OAM beams in free space. Subsequently, various fiber integrated polymer microlenses with sufficient optical performances induced by TPP have been reported, which demonstrate the potential of this technology. **Figure 1C** shows a collimation lens printed on the SMF (Gissibl et al., 2016b). The optical microscope image depicts that the polymer collimation lens appears as transparent as the fiber, and the smooth surfaces and the high quality of the photoresists make it possible to reach total transmittances of up to nearly 70% including the input and output coupling losses. Additionally, as shown in **Figure 1D**, a variety of ultra-compact compound lens systems with numerous refractive surfaces have been printed on the end face of SMF for endoscopy applications (Gissibl et al., 2016c). The lenses showed unprecedented performances and high optical quality with resolutions of up to 500 lp mm^{-1} for imaging applications, which makes it possible to provide high quality imaging on the micro-/nanoscale in numerous previously unavailable fields including optical fiber endoscopes and optical fiber microscopes. In addition to the extensive study of individual microlenses, optical fiber integrated

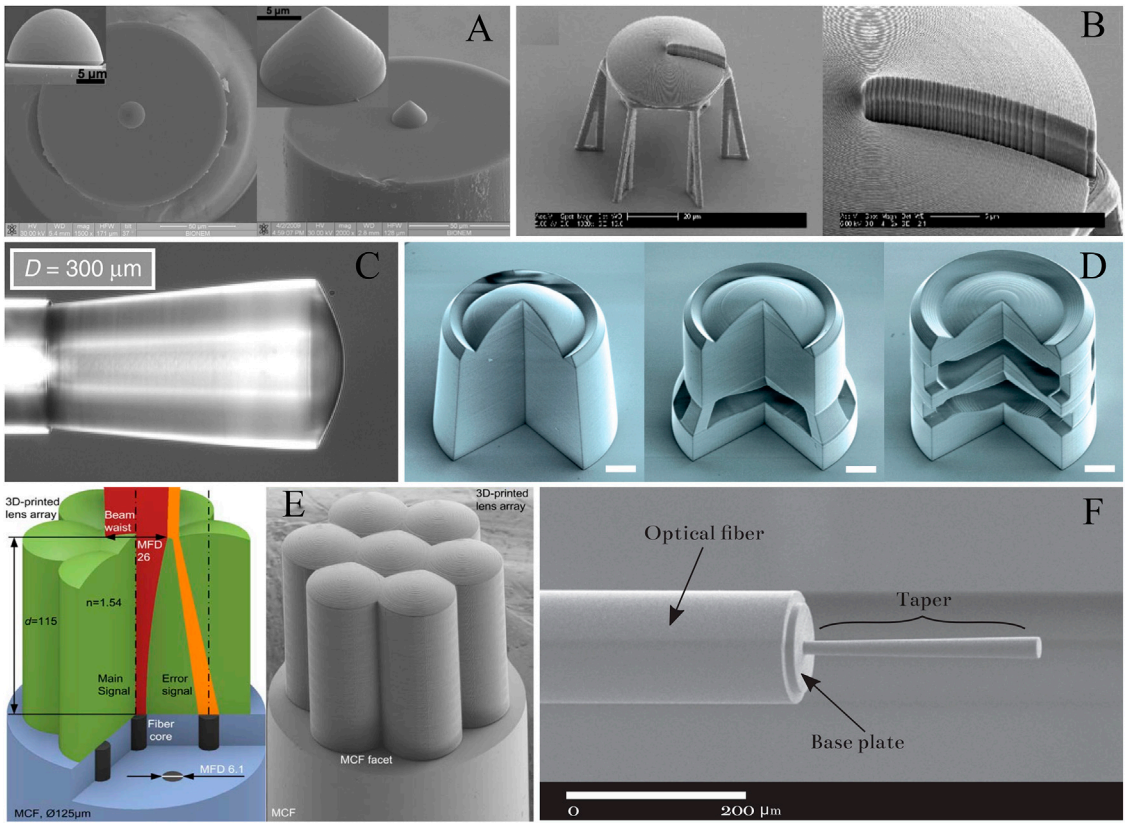

FIGURE 1 | Optical fiber integrated polymer microlenses printed by TPP. **(A)** Convergent lens and axicon lens fabricated on end face of SMF (Cojoc et al., 2010; Liberale et al., 2010). **(B)** Spherical lens with an azimuthal spiral phase plate on top for generating OAM beams in free space (Weiss and Marom, 2016). **(C)** Collimation lens printed on the top of SMF (Gissibl et al., 2016b). **(D)** Ultra-compact compound lens systems with numerous refractive surfaces for endoscopy applications (Gissibl et al., 2016c). **(E)** Microlens array printed on the top of single-mode and multi-core fiber for free-space light coupling (Dietrich et al., 2017). **(F)** Beam expansion taper for SMF-SMF coupling (Vanmol et al., 2019).

polymer microlens arrays have also been printed for some specific applications. For example, Dietrich et al. (2017) reported microlens array on the end face of a single-mode and multi-core fiber for free-space light coupling as shown in **Figure 1E**. The microlens array allowed the coupling of a single Gaussian beam to individual SMF with high efficiency of up to 73% (down to 1.4 dB loss) and provided an error signal that can be used as a feedback for an adaptive optics system, which paves the path to innovative multichannel optical devices. Meanwhile, the lenses for fiber-fiber coupling have also been studied. **Figure 1F** shows a beam expansion taper for SMF-SMF coupling by transmitting the fundamental mode adiabatically from a SMF to 3 times larger mode field area in physical contact expanded beam connectors (Vanmol et al., 2019). The trade-off between achievable insertion loss and misalignment tolerance relaxation was demonstrated by measuring a total insertion loss as low as 0.76 dB.

In addition to the polymer microlenses, the phase plates can also be fabricated induced by TPP. As shown in **Figure 2A**, a simple ring shaped phase mask was the first to be printed on the SMF end face. It was able to transform the nearly Gaussian fiber mode in a propagating beam profile with a central peak and side lobes, which could be used for the efficient coupling of high-order modes in optical waveguides (Cojoc et al., 2010; Liberale et al., 2010). With the further reduction of the feature size that can be fabricated by TPP technology, it is feasible to achieve unprecedented diffractive elements with low micrometer geometric size. As shown in **Figure 2B**, Gissibl et al., 2016a demonstrated a diffractive phase plate that was fabricated by ring-by-ring on the SMF end face for spatial intensity shaping. Based on this diffraction structure, the distribution of intensity emerged from an optical fiber could be spatially redistributed. Besides, the phase masks for the delivery of OAM light have also been printed. A spiral phase plate with 10 discrete steps has been fabricated on the top of SMF (Weber et al., 2017), as shown in **Figure 2C**. The OAM light up to a topological charge of $l = 1$, two and three was delivered, and the power throughputs of over 50% were obtained for all fibers used in the experiment. The diameter of the phase mask did not affect the performance due to the light propagating through the core passes only through the center of spiral phase plate, therefore, the time of fabrication can be reduced by using a smaller spiral phase plate diameter. This simple and easy integration approach offers a high potential for practical applications including optical trapping or manipulation. Additionally, Xie et al. (2018) reported an integrated (de)

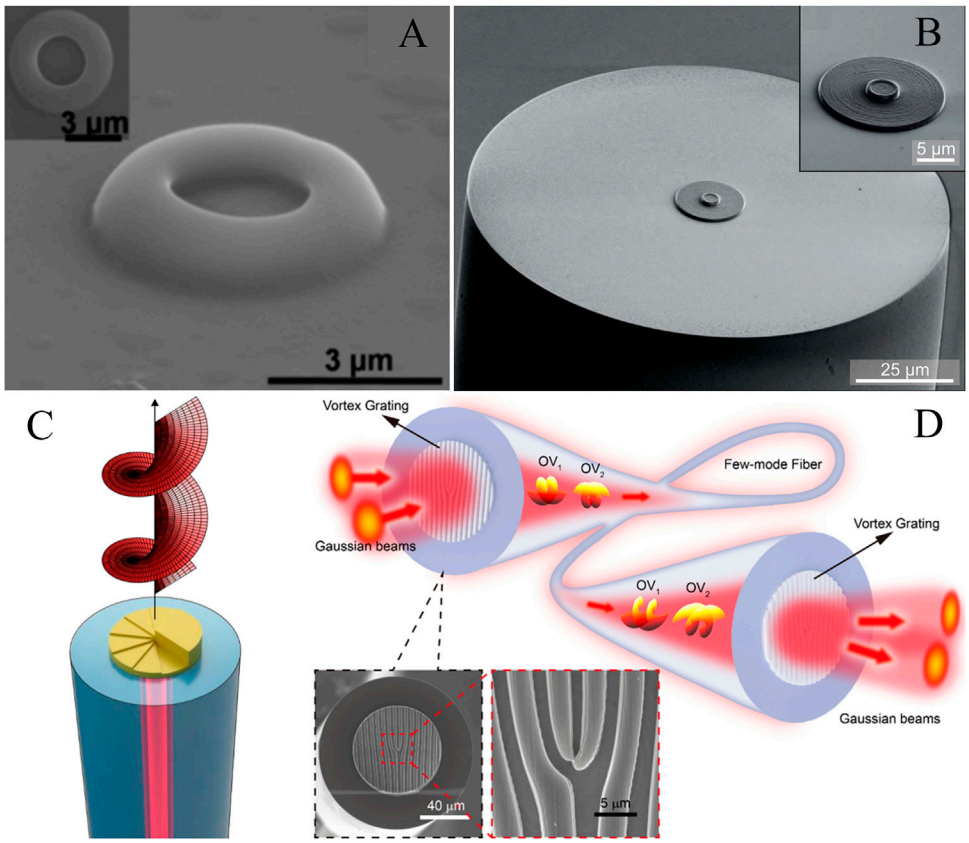

FIGURE 2 | Optical fiber integrated polymer phase plates printed by TPP. **(A)** Ring shaped phase mask printed on the SMF for efficient coupling (Cojoc et al., 2010; Liberale et al., 2010). **(B)** Diffractive phase plate fabricated by means of ring-by-ring printed on the SMF for spatial intensity shaping (Gissibl et al., 2016a). **(C)** Spiral phase plate with 10 discrete steps printed on the SMF for the efficient conversion of optical vortex beams carrying OAM (Weber et al., 2017). **(D)** Vortex grating as integrated (de) multiplexer attached onto the facets of a few-mode fiber (Xie et al., 2018).

multiplexer for OAM fiber communication. **Figure 2D** shows a polymer vortex grating that attached onto the facets of a few-mode fiber, which enabled the conversion of multiple Gaussian beams to multiple OAM. After coaxial propagation, these OAM modes were converted back to Gaussian-like beams in different directions. In addition to its ultra-compact size and low cost, the optical fiber integrated OAM (de)multiplexer also provided efficiency, flexibility, and a wide range of broadband responses. Therefore, it has promising applications in high-capacity OAM communications based on optical fiber.

For other fiber integrated polymer micro-optics printed by TPP, such as photonic crystal, surface-enhanced Raman scattering (SERS) and hybrid photonic integration devices, have also been widely explored. For example, as shown in **Figure 3A**, Willams et al. (2011) firstly reported the fabrication of woodpile photonic crystal structure on the fiber end face by TPP, which illustrates the ability of TPP to integrate directly onto fiber truly 3D structures with high degree of undercut and complex topology. Besides photonic crystal structures, a microstructured gradient-index antireflective coating with the complex contour was also printed on the fiber-tip (Kowalczyk et al., 2014), as shown in **Figure 3B**. The structure was composed of regular array of hemi-ellipsoidal protrusions that can significantly reduce the Fresnel reflection from the glass-air interface. The measurement result showed that the reflectivity was reduced by 30 times at 1,550 nm, and below 0.28% during 100 nm spectral band around the central wavelength. Additionally, the fabrication of optical fiber integrated SERS by TPP has been also realized. Xie et al. (2015) demonstrated a SERS radar structure based on MMF, which was composed of a parabolic mirror and a 3D spherical SERS body, as shown in **Figure 3C**. The Parabolic mirror with Au coating was used to focus the excitation laser on the SERS body and collect the Raman scattering light back into the optical fiber. The SERS body was composed of microscale trenches to increase the surface area of interaction with analytes. Such a device exhibited a detection limit of 10^{-6} mol/L for crystal violet in ethanol, which was comparable with high-quality Ag-based SERS fiber sensors. Recently, the fiber integrated SERS sensors have been upgraded to be used for practical biological analytes sensing. As shown in **Figure 3D**, a SERS consists of cross spike array was printed on the fiber tip for rapid detection of live *Escherichia coli* cells (Kim et al., 2020). A limit of detection of 10^{-7} mol/L (Rhodamine 6G) and an analytical enhancement factor of up

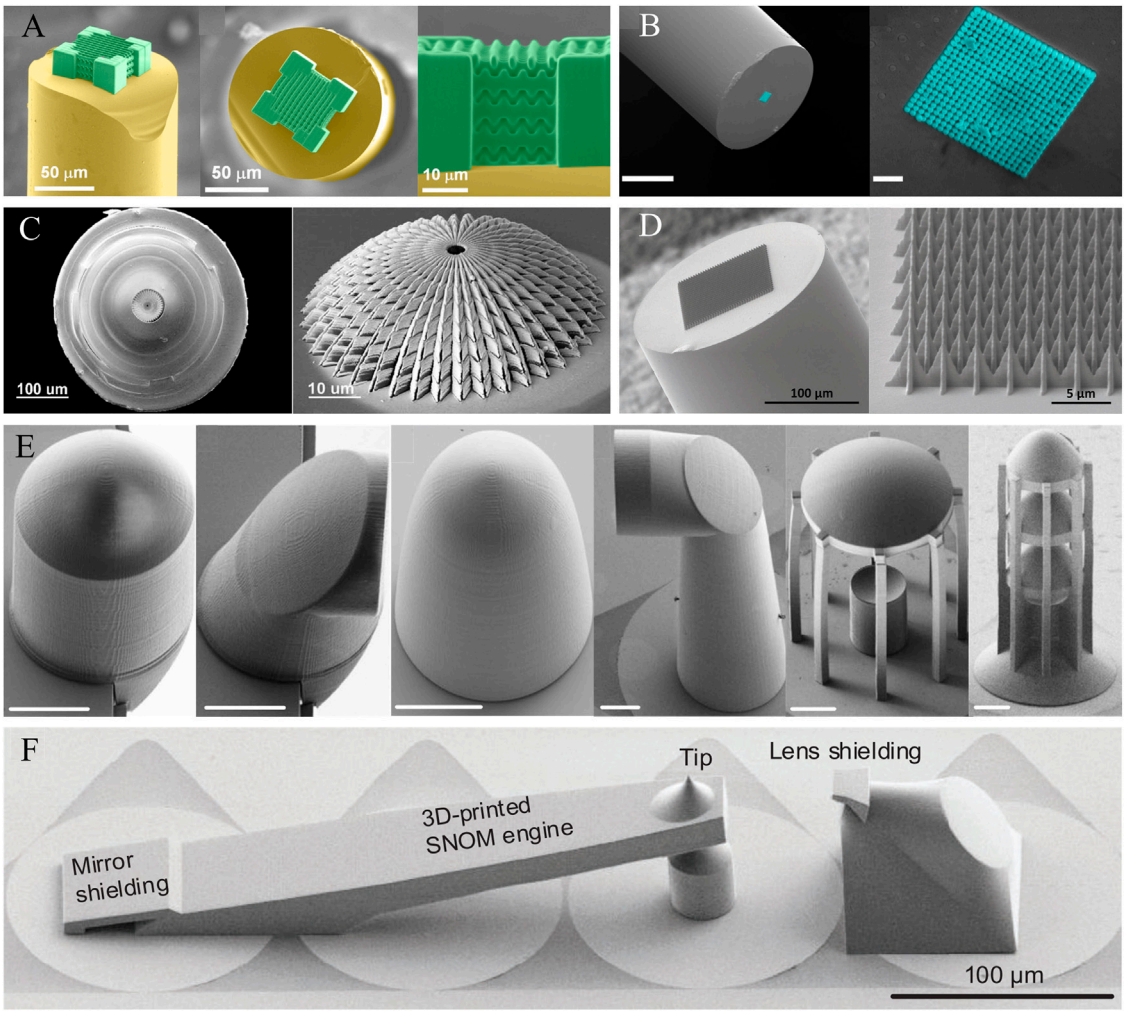

FIGURE 3 | Optical fiber integrated polymer micro-optics printed by TPP. **(A)** Woodpile photonic crystal structure printed on the SMF (Williams et al., 2011). **(B)** Microstructured gradient-index antireflective coating printed on the SMF for reduce the Fresnel reflection (Kowalczyk et al., 2014). **(C)** 3D SERS radar structure printed on MMF (Xie et al., 2015). **(D)** Fiber SERS probe with cross spike array for rapid detection of live bacteria (Kim et al., 2020). **(E)** Free-form lenses, free-form mirrors and beam expanders for the coupling between the optical fiber end face and the chip interface (Dietrich et al., 2018). **(F)** Scanning-probe microscope (SPM) with integrated optical actuation and read-out based on fiber array (Dietrich et al., 2020).

to 1,300 were obtained, and the feasibility of rapid bacteria detection was verified using integration times as low as 1 s. It is worth noting that this is the first demonstration of using SERS probes based fiber tip for the label-free detection of live bacteria. In addition to the development of micro-optics based on single fiber, TPP also has the excellent ability to fabricate elements on fiber-chip systems or multi-fiber platforms. For example, Dietrich et al. (2018) reported the fabrication of the couplers between the optical fiber end face and the chip interface by TPP, including free-form lenses, free-form mirrors and beam expanders, as shown in **Figure 3E**. This hybrid photonic integration coupling induced by TPP paves the way for automated assembly of photonic multi-chip systems with unprecedented performance and versatility. For multi-fiber integrated micro-optics, this group also demonstrated a highly compact scanning-probe microscopes (SPM) with integrated optical actuation and read-out (Dietrich et al., 2020), as shown in **Figure 3F**. The SPM engine was composed of cantilevers and probe tips, and integrates optical actuation and read-out by combining mirrors and lenses. The SPM engine offered the atomic step-height resolution suitable for operation both in air and in liquid. More importantly, this is the first complex integrated optical system based on multiple optical fibers upgraded by TPP technology, which would open the door to upgrading various traditional micro-optical systems with TPP technology in the future.

OPTICAL WAVEGUIDE DEVICES

Compared with the above fiber integrated micro-optics that mainly take advantage of high precision and flexibility of TPP, the research of optical waveguide devices relies more on the

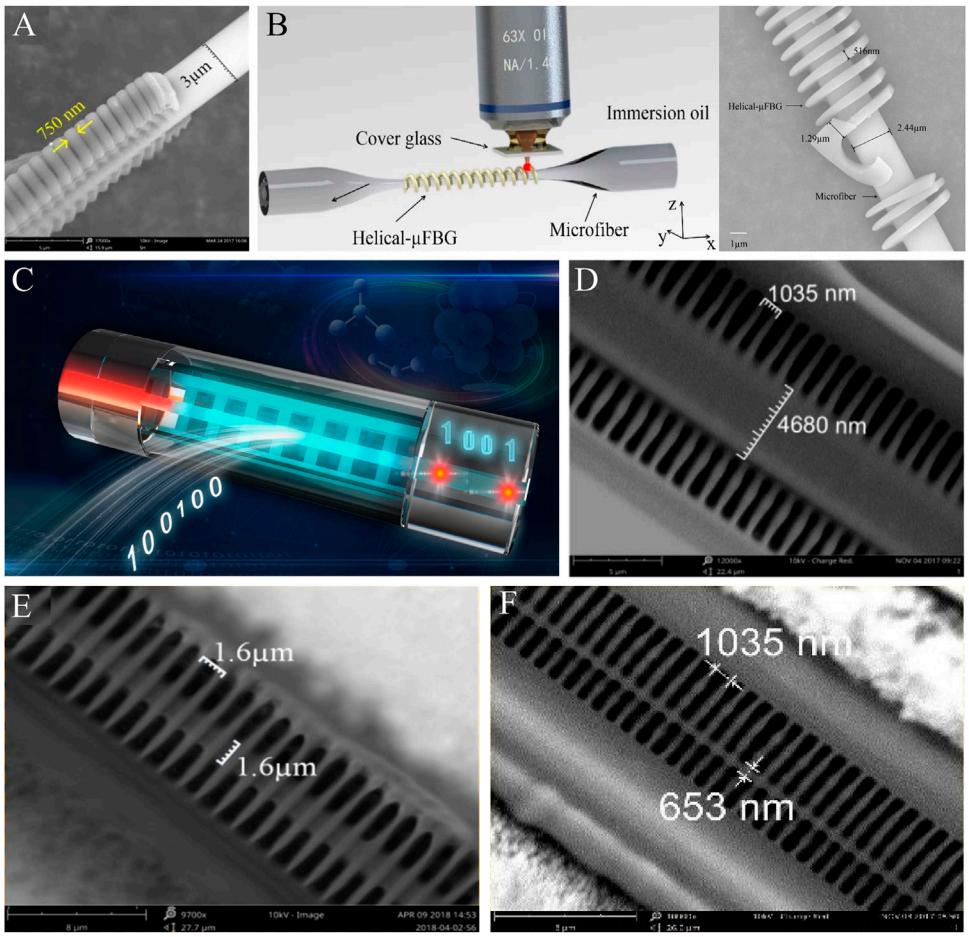

FIGURE 4 | Optical fiber integrated waveguides printed by TPP. **(A)** Microfiber surface integrated polymer FBG for RI sensing (Wang et al., 2018). **(B)** Microfiber surface integrated helical polymer FBG for RI sensing (Liao et al., 2019). **(C)** Schematic diagram of the integration of fiber interior polymer FBG (Liao et al., 2020). **(D)** Fiber interior integrated polymer FBG for temperature sensing (Li et al., 2018b). **(E)** Fiber interior integrated polymer multimode interferometer for temperature sensing (Li et al., 2018a). **(F)** High-speed all-optical modulator based on polymer nanofiber Bragg grating (Liao et al., 2020).

renewal of materials brought by TPP. Conventional optical fiber sensors, such as fiber Bragg gratings (FBG) (Majumder et al., 2008; Grobnic et al., 2015) and long-period fiber gratings (LPFG) (Zhong et al., 2014; Yin et al., 2015), are generally of limited sensitivity due to the low thermo-optical and thermal expansion coefficients of the silica material. Fortunately, the silica optical waveguide can be replaced by the polymer one printed by TPP, and its good physical parameters guarantee the improvement of sensor sensitivity. In the last ten years, the research in the field of optical waveguide devices induced by TPP was mainly focused on FBG, which could be divided into two integrated modes: fiber surface and fiber interior. For fiber surface integration, our group firstly reported a line-type polymer FBG that was printed on microfiber surface for the measurement of liquid refractive index (RI) (Wang et al., 2018), as shown in **Figure 4A**. Such a polymer FBG exhibited a maximum RI sensitivity of ~207 nm/RIU at 1.44. Successively, our group demonstrated a helical microfiber polymer FBG for RI sensing (Liao et al., 2019), as shown in **Figure 4B**. Compared with the line-type polymer FBG, the helical one showed better reflection spectrum and mechanical strength due to the enlarged contact area between the polymer grating and fiber surface. For fiber interior integration, our group proposed a suspended polymer FBG printed in a grooved silica tube, which was spliced between two SMFs. As shown in **Figure 4C**, the printed structure contained a pair of polymer bases for enhance structural stability and a polymer waveguide for guide light and several polymer grating segments for generate Bragg resonance (Liao et al., 2020). As shown in **Figure 4D**, the width of the polymer waveguide was optimized to 4.6 μm to excite the Bragg resonance with reduced propagation loss and multimode interference effect for highly sensitive temperature measurements (Li et al., 2018b). The measurement result showed a high sensitivity of −220 pm/°C, which was 10 times the sensitivity of FBG temperature sensors based on commercial silica fiber. Then, our group realized a multimode interferometer for high-sensitivity temperature measurement by reducing the width of the polymer waveguide to 1.6 μm (Li et al., 2018a), as shown in **Figure 4D**. The SMF was replaced by a thin-core fiber to

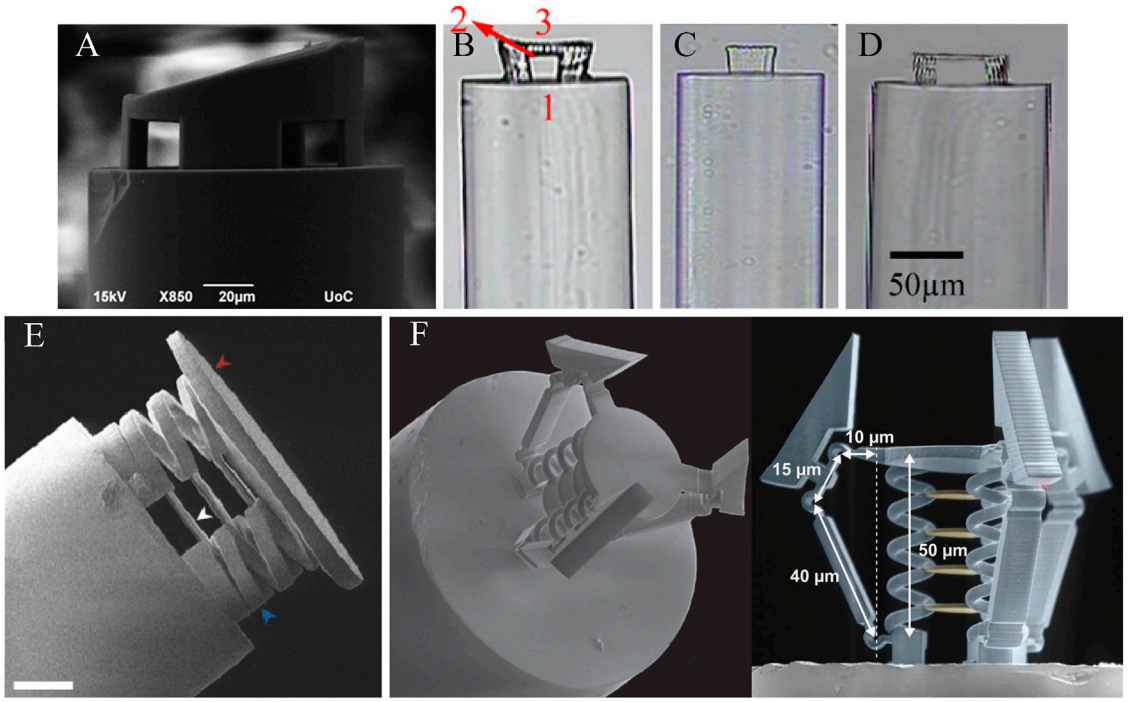

FIGURE 5 | Optical fiber integrated FPIs printed by TPP. **(A)** Open cavity FPI for vapor sensing (Melissinaki et al., 2015). **(B)** Open cavity FPI for simultaneous measurement of liquid RI and temperature (Li et al., 2015). **(C)** Liquid polymer filled FPI with sealed cavity for temperature sensing (Li et al., 2016a). **(D)** Open cavity FPI for acoustic sensing (Li et al., 2017a). **(E)** Microscale fiber force sensor (Thompson et al., 2018). **(F)** Force-sensitive microgripper (Power et al., 2018).

match the mode field of the polymer waveguide. It is worth noting that such an interferometer showed a high temperature sensitivity of ~6.4 nm/°C. Furthermore, an all-optical modulator was demonstrated by further reducing the diameter of the polymer waveguide to 653 nm (Liao et al., 2020), as shown in **Figure 4E**. The thermal expansion of polymer FBG by absorbing the pump light leads to the change of the effective RI, which gave rise to the shift of resonant wavelength. Therefore, the probe light could be modulated by spectral filtering. Such a device exhibited a fast temporal response of 176 ns and a good linear modulation of −45.43 pm/mW. Moreover, this work firstly employed Bragg resonance to realize a fiber-integrated all-optical modulator, which opened the door to realization of multifunctional lab-in-fiber devices.

OPTICAL MICRO-CAVITY

Optical micro-cavity is a very important sensing structure, which is well known for its applicability in many fields and rich kinds. Fabry–Pérot interferometer (FPI) is the most commonly used optical micro-cavity. In 2015, Melissinaki et al. (2015) reported an open-cavity FPI on fiber end face for sensing the vapors of common organic solvents. As shown in **Figure 5A**, there were several openings at the bottom of the cavity for wash away the residual photoresist and fill the vapors of common organic solvents, and the outer surface of the cavity was designed with a 20° inclination for avoid multi-beam interference. Such a sensor exhibited a detection limit of ethanol vapor concentration down to 4 ppm and a high sensitivity of ~1.5×10^3 nm/RIU. Similarly, an open-cavity ⊓-shaped FPI was demonstrated for simultaneous measurement of the liquid RI and temperature (Li et al., 2015), as shown in **Figure 5B**. Different from the FPI mentioned above, this sensor works with the multi-beam interference. The simultaneous measurement of RI and temperature were achieved by tracing the shifts of two dips in spectrum and calculating by the sensitivity matrix method. The two dips exhibited the RI sensitivities of 1,539 nm/RIU and 863 nm/RIU, and the temperature sensitivities of 451 pm/°C and 206 pm/°C, respectively. Then, this group increased the temperature sensitivity by filling the open cavity with liquid polymer and sealing it (Li et al., 2016a), as shown in **Figure 5C**. The temperature sensitivity was increased up to 877 pm/°C, which was more than three times as high as the sensitivity of solid cross-linking polymer cavity FPI due to the higher thermal expansion coefficient of the liquid polymer. Furthermore, as shown in **Figure 5D**, this group demonstrated a highly sensitive fiber acoustic sensor by reducing the thickness of the polymer film of the open cavity to 1.6 μm (Li et al., 2017a). This polymer film was easier to vibrate with a large deformation under the effect of acoustic. Such a fiber acoustic sensor exhibited an acoustic pressure sensitivity of 0.0508 ± 0.0052 nm/Pa at the acoustic frequency of 1 kHz. Recently, more complex structures based on fiber FPI have been printed nicely. Thompson et al. (2018) reported a microscale fiber-optic force sensor printed on the SMF end face, as show in **Figure 5E**. The sensor was

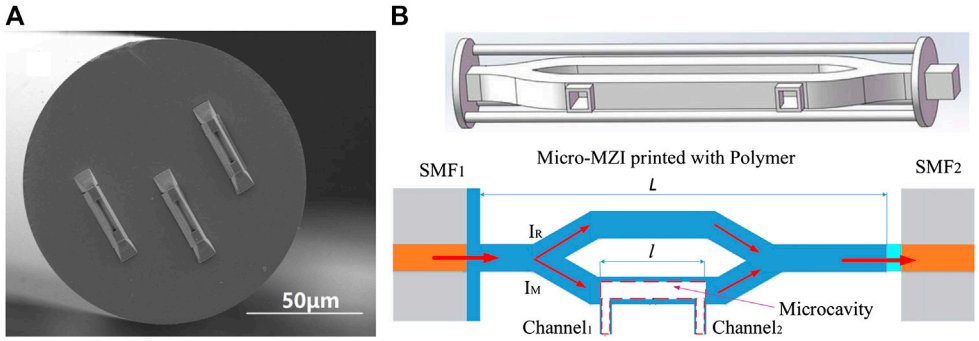

FIGURE 6 | Optical fiber integrated MZI printed by TPP. **(A)** Polymer MZI based on seven core fiber for liquid RI detection (Qi et al., 2017). **(B)** Optofluidic polymer MZI for liquid RI detection (Zhang et al., 2019a).

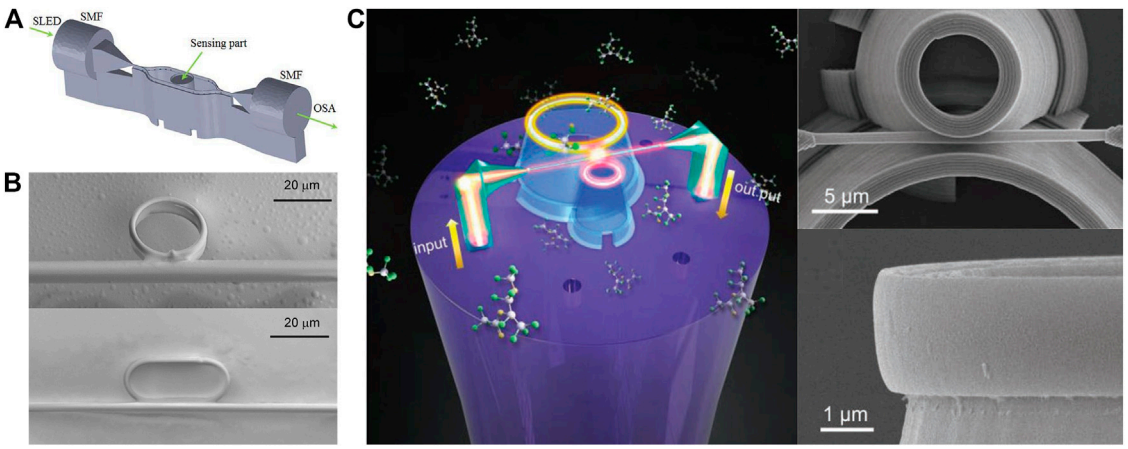

FIGURE 7 | Optical fiber integrated WGM resonators printed by TPP. **(A)** Fiber inline polymer WGM resonator for RI sensing (Wei and Krishnaswamy, 2016). **(B)** Fiber surface integrated polymer WGM resonators for high sensitivity temperature measurement (Li et al., 2019). **(C)** Polymer WGM resonator with high Q-factor based on SCF end face for vapor sensing (Zhang et al., 2019b).

composed of a series of thin plates and springs. When the thin plate on the top was extruded with external force, the space between the thin plates was reduced due to the spring shrinkage, and the length of the FPI cavity was changed. After calibration, the sensor can be used for force sensing over the range 0–50 μN with a measurement error of ~1.5 μN. In addition, this group upgraded it to a force-sensitive microgripper by adding three fingers (Power et al., 2018), as shown in **Figure 5F**. The microgripper could manipulate the objects of ~100 μm in length and breadth, and the axial force exerted could be adjusted in real time by tracking the interference spectrum. This device has significant potential for future sensing, cellular manipulation and microscale surgery due to the ability to manipulate soft/fragile microscale objects in real time.

For MZIs, Liu et al. (2017) reported a MZI based on a polymer waveguide integrated in fiber micro-cavity. Such a device exhibited a perfect interference spectrum with a fringe visibility of 25 dB, and obtained a high temperature sensitivity of 447 pm/°C with a linearity of 99.7%. Besides, Qi et al. (2017) demonstrated a MZI based on SCF for liquid RI detection. As shown in **Figure 6A**, the sensor was designed as a trapezoid body with an inverted wedge groove in the center, two sides were used as prisms to turn light paths, and the polymer and the groove in the middle played the roles of reference and sensing arms. The novel MZI exhibited a high sensitivity of 1,616 nm/RIU, and realized an ultra-compact device with multiple sensors integrated. Additionally, a specially designed optofluidic MZI has also been reported (Zhang et al., 2019a). As shown in **Figure 6B**, the MZI was composed of two consecutive Y-splitters. A solid polymer and a hollow polymer with channels for liquid in and out as the reference and sensing arm, respectively. The experiment result showed a high RI sensitivity of 593.75 nm/RIU. The fabrication of this unprecedented MZI structure by using TPP is of great significance for broadening the application field of optical fiber MZIs.

Owing to TPP has the capability to print high smooth surface and accurately grasp the structure position, it is very suitable for the fabrication of fiber integrated WGM resonators. For example,

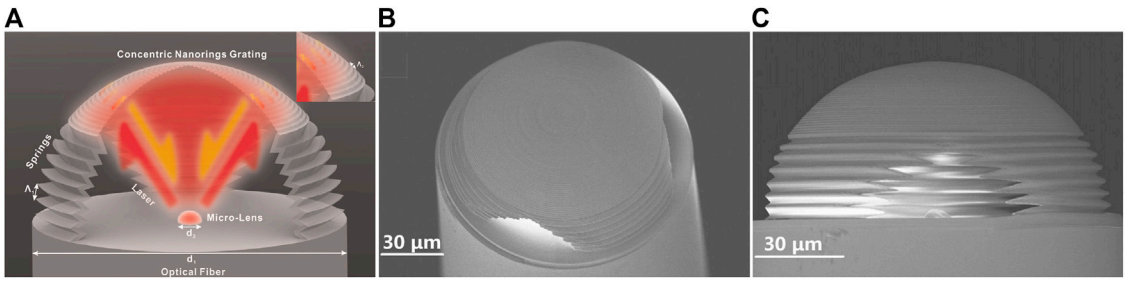

FIGURE 8 | Optical fiber integrated microphone printed by TPP (Wang et al., 2015). **(A)** Schematic illustration of the 3D design. **(B)** Top view of the fiber microphone. **(C)** Side view of the fiber microphone.

as shown in **Figure 7A**, Wei and Krishnaswamy (2016) demonstrated a polymer WGM sensor that consists of tapered waveguides, Y-splitters, parallel waveguides and micro-cylinder. The highest experimental Q-factor of 6,400.8 was obtained at 1,536 nm wavelength, and it could be inexpensively fabricated as an integrated device for accurate measurements of RI of liquids due to the reasonably high sensitivity of 154.84 nm/RIU. Additionally, our group reported the WGM resonators based on microfiber for highly sensitive temperature measurements (Li et al., 2019). As shown in **Figure 7B**, the ring structure (circle and racetrack) was printed to the side of microfiber, and the light was coupled to the ring resonator for WGM resonance due to the strong evanescent field of microfiber. Although such a device only obtained a Q-factor of 1.9×10^3, it exhibited a high temperature sensitivity of 1.68 nm/°C, which improved one order of magnitudes than PDMS microsphere and glass microsphere. Furthermore, Zhang et al., 2019b demonstrated a high Q-factor polymer WGM resonator integrated on SCF for vapor sensing. As show in **Figure 7C**, the resonator was composed of micropillars, prisms, tapers, a waveguide and ring resonators on the end facet of a cleaved SCF. The smooth surface of ring resonators was helpful to improve Q-factor. The spectrum exhibited a Q-factor of up to 1.2×10^5, which was the highest value for fiber integrated WGM resonator fabricated by TPP.

More complex micro-cavity structures have been achieved by TPP. For example, Wang et al. (2015) reported fiber microphone with concentric nanorings grating and microsprings structured diaphragm, as shown in **Figure 8**. The vibration of the resonant grating waveguide structure under impact of sound pressure would change the intensity of the light reflected back to the fiber, and the microsprings make the diaphragm be more sensitive to the pressure changing in media caused by sound. Acoustic inspections showed that such a device could detect the weak sound in air with frequency band from 400 to 2000 Hz.

CONCLUSION AND PERSPECTIVE

So far, a variety of fiber integrated functional micro-/nanostructures induced by TPP have been demonstrated, including micro-optics, optical waveguide device and optical micro-cavity. With the increasing demands of micro-/nanoscale optical imaging, shaping, optical manipulation and sensing, the ultra-compact devices based on fiber integrated functional micro-/nanostructures will have great application potential. The combination of TPP and the concept of "Lab on fiber" not only gives full play to the advantages of fiber as an ultra-compact optical coupling platform, but also makes it possible to manufacture unprecedented micro-/nanostructures. As TPP technology advances, new processing methods and materials, as well as new functional structures, will continue to bestow new opportunities for fiber devices. To take a glimpse into the future, the application of fiber integrated devices can be expanded by functionalizing polymer materials (eg., Doped the photoresist with functional particles such as magnetic nanoparticles, carbon nanotubes and biological quantum dots). On one hand, the fabrication of micro-/nanostructures inherits the advantages of high precision and flexibility. On the other hand, the printed structures add special properties such as mechanical, electrical and chemical, which provides the possibility to expand the application of fiber integrated device in the fields of micromechanics, microelectronics and biology. Therefore, we believe that the combination of TPP and the concept of "Lab on fiber" could open an exciting path for the development of micro/nano functional devices.

AUTHOR CONTRIBUTIONS

CX and CL drafted the manuscript. ZL, KY, MZ, YZ, and YW were involved in the data analysis and discussions.

FUNDING

This work was supported by the Natural Science Foundation of Guangdong Province (2018B030306003, 2020A0505100066), the Science and Technology Innovation Commission of Shenzhen (JCYJ20180507184503128), National Natural Science Foundation of China (61905162).

REFERENCES

Alsharif, N., Burkatovsky, A., Lissandrello, C., Jones, K. M., White, A. E., and Brown, K. A. (2018). Design and realization of 3D printed AFM probes. *Small* 14, 1800162. doi:10.1002/smll.201800162

Bianchi, S., Rajamanickam, V. P., Ferrara, L., Fabrizio, E. D., Liberale, C., and Leonardo, R. D. (2013). Focusing and imaging with increased numerical apertures through multimode fibers with micro-fabricated optics. *Opt. Lett.* 38, 4935–4938. doi:10.1364/OL.38.004935

Cabrini, S., Liberale, C., Cojoc, D., Carpentiero, A., Prasciolu, M., Mora, S., et al. (2006). Axicon lens on optical fiber forming optical tweezers, made by focused ion beam milling. *Microelectron. Eng.* 83, 804–807. doi:10.1016/j.mee.2006.01.247

Cojoc, G., Liberale, C., Candeloro, P., Gentile, F., Das, G., Angelis, F. D., et al. (2010). Optical micro-structures fabricated on top of optical fibers by means of two-photon photopolymerization. *Microelectron. Eng.* 87, 876–879. doi:10.1016/j.mee.2009.12.046

Dianov, E. M. (2012). Bismuth-doped optical fibers: a challenging active medium for near-IR lasers and optical amplifiers. *Light Sci. Appl.* 1, e12. doi:10.1038/lsa.2012.12

Dietrich, P.-I., Blaicher, M., Reuter, I., Billah, M., Hoose, T., Hofmann, A., et al. (2018). *In situ* 3D nanoprinting of free-form coupling elements for hybrid photonic integration. *Nat. Photonics* 12, 241–247. doi:10.1038/s41566-018-0133-4

Dietrich, P.-I., Göring, G., Trappen, M., Blaicher, M., Freude, W., Schimmel, T., et al. (2020). 3D-printed scanning-probe microscopes with integrated optical actuation and read-out. *Small* 15, 1904695. doi:10.1002/smll.201904695

Dietrich, P.-I., Harris, R. J., Blaicher, M., Corrigan, M. K., Morris, T. J., Freude, W., et al. (2017). Printed freeform lens arrays on multi-core fibers for highly efficient coupling in astrophotonic systems. *Opt. Express* 25, 18288–18295. doi:10.1364/OE.25.018288

Gissibl, T., Schmid, M., and Giessen, H. (2016a). Spatial beam intensity shaping using phase masks on single-mode optical fibers fabricated by femtosecond direct laser writing. *Optica* 3, 448–451. doi:10.1364/OPTICA.3.000448

Gissibl, T., Thiele, S., Herkommer, A., and Giessen, H. (2016b). Sub-micrometre accurate free-form optics by three-dimensional printing on single-mode fibres. *Nat. Commun.* 7, 11763. doi:10.1038/ncomms11763

Gissibl, T., Thiele, S., Herkommer, A., and Giessen, H. (2016c). Two-photon direct laser writing of ultracompact multi-lens objectives. *Nat. Photonics* 10, 554–560. doi:10.1038/nphoton.2016.121

Grobnic, D., Mihailov, S. J., Ballato, J., and Dragic, P. D. (2015). Type I and II Bragg gratings made with infrared femtosecond radiation in high and low alumina content aluminosilicate optical fibers. *Optica* 2, 313–322. doi:10.1364/OPTICA.2.000313

Han, J., Zhang, Y., Liao, C., Jiang, Y., Wang, Y., Lin, C., et al. (2020). Fiber-interface directional coupler inscribed by femtosecond laser for refractive index measurements. *Opt. Express* 28, 14263–14270. doi:10.1364/OE.390674

Hippler, M., Lemma, E. D., Bertels, S., Blasco, E., Kowollik, C. B., Wegener, M., et al. (2019). 3D scaffolds to study basic cell biology. *Adv. Mater.* 31, 1808110. doi:10.1002/adma.201808110

Hou, M., Yang, K., He, J., Xu, X., Ju, S., Guo, K., et al. (2018). Two-dimensional vector bending sensor based on seven-core fiber Bragg gratings. *Opt. Express* 26, 23770–23781. doi:10.1364/OE.26.023770

Hou, Z., Xiong, X., Cao, J., Chen, Q., Tian, Z., Ren, X., et al. (2019). On-chip polarization rotators. *Adv. Optical Mater.* 7, 1900129. doi:10.1002/adom.201900129

Jain, C., Braun, A., Gargiulo, J., Jang, B., Li, G., Lehmann, H., et al. (2019). Hollow core light cage: trapping light behind bars. *ACS Photonics* 6, 649–658. doi:10.1021/acsphotonics.8b01428

Johnson, E. G., Stack, J., Suleski, T. J., Koehler, C., and Delaney, W. (2003). Fabrication of micro optics on coreless fiber segments. *Appl. Opt.* 42, 785. doi:10.1364/AO.42.000785

Kanamori, Y., Okochi, M., and Hane, K. (2013). Fabrication of antireflection subwavelength gratings at the tips of optical fibers using UV nanoimprint lithography. *Opt. Express* 21, 322–328. doi:10.1364/OE.21.000322

Kawata, S., Sun, H., Tanaka, T., and Takada, K. (2001). Finer features for functional microdevices. *Nature* 412, 697–698. doi:10.1038/35089130

Kim, J. A., Wales, D. J., Thompson, A. J., and Yang, G. (2020). Fiber-optic SERS probes fabricated using two-photon polymerization for rapid detection of bacteria. *Adv. Optical Mater.* 8, 1901934. doi:10.1002/adom.201901934

Kostovski, G., Chinnasamy, U., Jayawardhana, S., Stoddart, P. R., and Mitchell, A. (2011). Sub-15nm optical fiber nanoimprint lithography: a parallel, self-aligned and portable approach. *Adv. Mater.* 23, 531–535. doi:10.1002/adma.201002796

Kowalczyk, M., Haberko, J., and Wasylczyk, P. (2014). Microstructured gradient-index antireflective coating fabricated on a fiber tip with direct laser writing. *Opt. Express* 22, 12545–12550. doi:10.1364/OE.22.012545

Lee, B. (2003). Review of the present status of optical fiber sensors. *Opt. Fiber Technol.* 9, 57–79. doi:10.1016/S1068-5200(02)00527-8

Li, C., Liao, C., Wang, J., Gan, Z., and Wang, Y. (2018a). Femtosecond laser microprinting of a polymer optical fiber interferometer for high-sensitivity temperature measurement. *Polymers* 10, 1192. doi:10.3390/polym10111192

Li, C., Liao, C., Wang, J., Li, Z., Wang, Y., He, J., et al. (2018b). Femtosecond laser microprinting of a polymer fiber Bragg grating for high-sensitivity temperature measurements. *Opt. Lett.* 43, 3409–3412. doi:10.1364/OL.43.003409

Li, M., Liu, Y., Gao, R., Li, Y., Zhao, X., and Qu, S. (2016a). Ultracompact fiber sensor tip based on liquid polymer-filled Fabry-Perot cavity with high temperature sensitivity. *Sens. Actuator B-Chem.* 233, 496–501. doi:10.1016/j.snb.2016.04.121

Li, Z., Liao, C., Song, J., Wang, Y., Zhu, F., Wang, Y., et al. (2016b). Ultrasensitive magnetic field sensor based on an in-fiber Mach-Zehnder interferometer with a magnetic fluid component. *Photon. Res.* 4, 197–201. doi:10.1364/PRJ.4.000197

Li, M., Liu, Y., Zhao, X., Gao, R., Li, Y., and Qu, S. (2017a). High sensitivity fiber acoustic sensor tip working at 1550 nm fabricated by two-photon polymerization technique. *Sens. Actuator A Phys.* 260, 29–34. doi:10.1016/j.sna.2017.03.040

Li, Z., Liao, C., Chen, D., Song, J., Jin, W., Peng, G., et al. (2017b). Label-free detection of bovine serum albumin based on an in-fiber Mach-Zehnder interferometric biosensor. *Opt. Express* 25, 17105–17113. doi:10.1364/OE.25.017105

Li, M., Liu, Y., Zhao, X., Qu, S., and Li, Y. (2015). Miniature ⊓-shaped polymer fiber tip for simultaneous measurement of the liquid refractive index and temperature with high sensitivities. *J. Opt.* 17, 105701. doi:10.1088/2040-8978/17/10/105701

Li, Z., Liao, C., Wang, J., Li, Z., Zhou, P., Wang, Y., et al. (2019). Femtosecond laser microprinting of a fiber whispering gallery mode resonator for highly-sensitive temperature measurements. *J. Lightwave Technol.* 37, 1241–1245. doi:10.1109/JLT.2019.2890991

Liao, C., Li, C., Wang, C., Wang, Y., He, J., Liu, S., et al. (2020). High-speed all-optical modulator based on a polymer nanofiber Bragg grating printed by femtosecond laser. *ACS Appl. Mater. Interfaces* 12, 1465–1473. doi:10.1021/acsami.9b16716

Liao, C., Yang, K., Wang, J., Bai, Z., Gan, Z., and Wang, Y. (2019). Helical microfiber Bragg grating printed by femtosecond laser for refractive index sensing. *IEEE Photon. Technol. Lett.* 31, 971–974. doi:10.1109/LPT.2019.2912634

Liberale, C., Cojoc, G., Candeloro, P., Das, G., Gentile, F., Angelis, F. D., et al. (2010). Micro-optics fabrication on top of optical fibers using two-photon lithography. *IEEE Photon. Technol. Lett.* 22, 474–476. doi:10.1109/LPT.2010.2040986

Lin, C., Liao, C., Zhang, Y., Xu, L., Wang, Y., Fu, C., et al. (2018). Optofluidic gutter oil discrimination based on a hybrid-waveguide coupler in fibre. *Lab Chip* 18, 595–600. doi:10.1039/c8lc00008e

Liu, S., Sun, Z., Zhang, L., Fu, C., Liu, Y., Liao, C., et al. (2018). Strain-based tunable optical microresonator with an in-fiber rectangular air bubble. *Opt. Lett.* 43, 4077–4080. doi:10.1364/OL.43.004077

Liu, Y., Li, M., Zhao, P., Wang, X., and Qu, S. (2017). High sensitive temperature sensor based on a polymer waveguide integrated in an optical fibre micro-cavity. *J. Opt.* 20, 015801. doi:10.1088/2040-8986/aa95de

Liu, Z., Jiang, X., Li, Y., Xiao, Y., Wang, L., Ren, J., et al. (2013). High-Q asymmetric polymer microcavities directly fabricated by two-photon polymerization. *Appl. Phys. Lett.* 102, 221108. doi:10.1063/1.4809724

Majumder, M., Gangopadhyay, T. K., Chakraborty, A. K., and Dasgupta, K. (2008). Fiber Bragg gratings in structural health monitoring-present status and applications. *Sens. Actuators A* 147, 150–164. doi:10.1016/j.sna.2008.04.008

Melissinaki, V., Farsari, M., and Pissadakis, S. (2015). A fiber-endface, fabry–perot vapor microsensor fabricated by multiphoton polymerization. *IEEE J. Sel. Top. Quant.* 21, 5600110. doi:10.1109/JSTQE.2014.2381463

Nocentini, S., Martella, D., Parmeggiani, C., Zanotto, S., and Wiersma, D. S. (2018). Structured optical materials controlled by light. *Adv. Optical Mater.* 6, 1800167. doi:10.1002/adom.201800167

Ovsianikov, A., Chichkov, B., Mente, P., Monteiro-Riviere, N. A., Doraiswamy, A., and Narayan, R. J. (2007). Two photon polymerization of polymer–ceramic hybrid materials for transdermal drug delivery. *Int. J. Appl. Ceram. Technol.* 4, 22–29. doi:10.1111/j.1744-7402.2007.02115.x

Power, M., Thompson, A. J., Anastasova, S., and Yang, G. Z. (2018). A monolithic force sensitive 3D microgripper fabricated on the tip of an optical fiber using 2-photon polymerization, *Small* 14, 1703964. doi:10.1002/smll.201703964

Prasciolu, M., Cojoc, D., Cabrini, S., Businaro, L., Candeloro, P., Tormen, M., et al. (2003). Design and fabrication of on-fiber diffractive elements for fiber-waveguide coupling by means of e-beam lithography. *Microelectron. Eng.* 67-68, 169–174. doi:10.1016/S0167-9317(03)00068-6

Presby, H. M., Benner, A. F., and Edwards, C. A. (1990). Laser micromachining of efficient fiber microlenses. *Appl. Opt.* 29, 2692-631. doi:10.1364/AO.29.002692

Qi, Y., Zhang, S., Feng, S., Wang, X., Sun, W., Ye, J., et al. (2017). "Integrated Mach-Zehnder interferometer on the end facet of multicore fiber for refractive index sensing application," in Proceedings of SPIE 10623, 2017 International Conference on Optical Instruments and Technology: IRMMW-THz Technologies and Applications, 106230T, 12 January 2018. doi:10.1117/12.2302441

Richardson, D. J., Fini, J. M., and Nelson, L. E. (2013). Space-division multiplexing in optical fibres. *Nat. Photon* 7, 354–362. doi:10.1038/NPHOTON.2013.94

Sanghera, J., Florea, C., Busse, L., Shaw, B., Miklos, F., and Aggarwal, I. (2010). Reduced Fresnel losses in chalcogenide fibers by using anti-reflective surface structures on fiber end faces. *Opt. Express* 18, 26760–26768. doi:10.1364/OE.18.026760

Schiappelli, F., Kumar, R., Prasciolu, M., Cojoc, D., Cabrini, S., Vittorio, M. D., et al. (2004). Efficient fiber-to-waveguide coupling by a lens on the end of the optical fiber fabricated by focused ion beam milling. *Microelectron. Eng.* 73-74, 391–404. doi:10.1016/j.mee.2004.02.077

Serbin, J., Egbert, A., Ostendorf, A., Chichkov, B. N., Houbertz, R., Domann, G., et al. (2003). Femtosecond laser-induced two-photon polymerization of inorganic–organic hybrid materials for applications in photonics. *Opt. Lett.* 28, 301–303. doi:10.1364/OL.28.000301

Spagnolo, B., Brunetti, V., Leménager, G., Luca, E. D., Sileo, L., Pellegrino, T., et al. (2015). Three-dimensional cage-like microscaffolds for cell invasion studies, *Sci. Rep.* 5, 10531. doi:10.1038/srep10531

Thompson, A. J., Power, M., and Yang, G. (2018). Micro-scale fiber-optic force sensor fabricated using direct laser writing and calibrated using machine learning. *Opt. Express* 26, 14186–14200. doi:10.1364/OE.26.014186

Tian, Y., Zhang, Y., Ku, J., He, Y., Xu, B., Chen, Q., et al. (2010). High performance magnetically controllable microturbines. *Lab Chip* 10, 2902–2905. doi:10.1039/c005277aGoogle Scholar

Tian, Z., Cao, X., Yao, W., Li, P., Yu, Y., Li, G., et al. (2016). Hybrid refractive–diffractive optical vortex microlens. *IEEE Photon. Technol. Lett.* 28, 2299–2302. doi:10.1109/LPT.2016.2591238

Vanmol, K., Tuccio, S., Panapakkam, V., Thienpont, H., Watté, J., and Erps, J. V. (2019). Two-photon direct laser writing of beam expansion tapers on single-mode optical fibers. *Opt. Laser Technol.* 112, 292–298. doi:10.1016/j.optlastec.2018.11.028

Wakaki, M., Komachi, T., and Kanai, G. (1998). Microlenses and microlens arraysformed on a glass plate by use of a CO_2 laser. *Appl. Opt.* 37, 627–631. doi:10.1364/AO.37.000627

Wang, H., Xie, Z., Zhang, M., Cui, H., He, J., Feng, S., et al. (2015). A miniaturized optical fiber microphone with concentric nanorings grating and microsprings structured diaphragm. *Opt. Laser Technol.* 78, 110–115. doi:10.1016/j.optlastec.2015.08.009

Wang, J., He, Y., Xia, H., Niu, L., Zhang, R., Chen, Q., et al. (2010). Embellishment of microfluidic devices via femtosecond laser micronanofabrication for chip functionalization. *Lab Chip* 10, 1993–1996. doi:10.1039/c003264f

Wang, J., Lin, C., Liao, C., Gan, Z., Li, Z., Liu, S., et al. (2018). Bragg resonance in microfiber realized by two-photon polymerization. *Opt. Express* 26, 3732–3737. doi:10.1364/OE.26.003732

Wang, Y. (2006). Asymmetric long period fiber gratings fabricated by use of CO_2 laser to carve periodic grooves on the optical fiber. *Appl. Phys. Lett.* 89, 151105. doi:10.1063/1.2360253

Wang, Y. (2010). Review of long period fiber gratings written by CO_2 laser. *J. Appl. Phys.* 108, 081101. doi:10.1063/1.3493111

Weber, K., Hütt, F., Thiele, S., Gissibl, T., Herkommer, A., and Giessen, H. (2017). Single mode fiber based delivery of OAM light by 3D direct laser writing. *Opt. Express* 25, 19672–19679. doi:10.1364/OE.25.019672

Wei, H., and Krishnaswamy, S. (2016). Direct laser writing polymer micro-resonators for refractive index sensors. *IEEE Photon. Technol. Lett.* 28, 2819–2822. doi:10.1109/LPT.2016.2623814

Weiss, I., and Marom, D. M. (2016). Direct 3D nanoprinting on fiber tip of collimating lens and OAM mode converter in one compound element. *Proc. Opt. Fiber Commun. Conf.* 1–3. doi:10.1364/OFC.2016.Th3E.2

Williams, H. E., Freppon, D. J., Kuebler, S. M., Rumpf, R. C., and Melino, M. A. (2011). Fabrication of three-dimensional micro-photonic structures on the tip of optical fibers using SU-8. *Opt. Express* 19, 22910–22922. doi:10.1364/OE.19.022910

Wu, D., Chen, Q., Niu, L., Wang, J., Wang, J., Wang, R., et al. (2009). Femtosecond laser rapid prototyping of nanoshells and suspending components towards microfluidic devices. *Lab Chip* 9, 2391–2394. doi:10.1039/b902159k

Xie, Z., Feng, S., Wang, P., Zhang, L., Ren, X., Cui, L., et al. (2015). Demonstration of a 3D radar-like SERS sensor micro- and nanofabricated on an optical fiber. *Adv. Optical Mater.* 3, 1232–1239. doi:10.1002/adom.201500041

Xie, Z., Gao, S., Lei, T., Feng, S., Zhang, Y., Li, F., et al. (2018). Integrated (de) multiplexer for orbital angular momentum fiber communication. *Photonics Res.* 6, 743–749. doi:10.1364/PRJ.6.000743

Yang, X., Ileri, N., Larson, C. C., Carlson, T. C., Britten, J. A., Chang, A. S. P., et al. (2012). Nanopillar array on a fiber facet for highly sensitive surface-enhanced Raman scattering. *Opt. Express* 20, 24819–24826. doi:10.1364/OE.20.024819

Yin, G., Wang, Y., Liao, C., Sun, B., Liu, Y., Liu, S., et al. (2015). Simultaneous refractive index and temperature measurement with LPFG and liquid-filled PCF. *IEEE Photon. Technol. Lett.* 27, 375–378. doi:10.1109/LPT.2014.2375337

Zhang, D., Wei, H., and Krishnaswamy, S. (2019a). 3D printing optofluidic mach-zehnder interferometer on a fiber tip for refractive index sensing. *IEEE Photon. Technol. Lett.* 31, 1725–1728. doi:10.1109/LPT.2019.2943897

Zhang, S., Tang, S., Feng, S., Xiao, Y., Cui, W., Wang, X., et al. (2019b). High-Q polymer microcavities integrated on a multicore fiber facet for vapor sensing. *Adv. Optical Mater.* 7 (20), 1900602. doi:10.1002/adom.201900602

Zhang, Y., Liao, C., Lin, C., Shao, Y., Wang, Y., and Wang, Y. (2019c). Surface plasmon resonance refractive index sensor based on fiber-interface waveguide inscribed by femtosecond laser. *Opt. Lett.* 44, 2434–2437. doi:10.1364/OL.44.002434

Zhang, Y., Lin, C., Liao, C., Yang, K., Li, Z., and Wang, Y. (2018). Femtosecond laser-inscribed fiber interface Mach–Zehnder interferometer for temperatureinsensitive refractive index measurement. *Opt. Lett.* 43, 4421–4424. doi:10.1364/OL.43.004421

Zhao, J., Cao, S., Liao, C., Wang, Y., Wang, G., Xu, X., et al. (2016). Surface plasmon resonance refractive sensor based on silver-coated side-polished fiber. *Sens. Actuator B-Chem.* 230, 206–211. doi:10.1016/j.snb.2016.02.020

Zhong, X., Wang, Y., Qu, J., Liao, C., Liu, S., Tang, J., et al. (2014). High-sensitivity strain sensor based on inflated long period fiber grating. *Opt. Lett.* 39, 5463–5466. doi:10.1364/OL.39.005463

Conflict of Interest: The authors declare that the research was conducted in the absence of any commercial or financial relationships that could be construed as a potential conflict of interest.